ChemComm

View Online / Journal Homepage
Dynamic Article Links

Cite this: DOI: 10.1039/c2cc35379b

www.rsc.org/chemcomm

COMMUNICATION

Oxygen evolution at functionalized carbon surfaces: a strategy for immobilization of molecular water oxidation catalysts†

Lianpeng Tong,[a] Mats Göthelid[b] and Licheng Sun*[ac]

Received 25th July 2012, Accepted 22nd August 2012
DOI: 10.1039/c2cc35379b

A molecular Ru(II) water oxidation catalyst was immobilized on a conductive carbon surface through a covalent bond, and its activity was maintained at the same time. The method can be applied to other materials and may inspire development of artificial photosynthesis devices.

Promising progress has been made on the development of molecular catalysts for water oxidation ($2H_2O \rightarrow O_2 + 4H^+ + 4e^-$) which is the critical and fundamental reaction of solar-energy conversion in both natural and artificial photosynthetic systems.[1,2] One of the latest breakthroughs in the field of water oxidation catalysis is the discovery of ruthenium and first-row transition-metal based complexes as highly efficient water oxidation catalysts (WOCs).[3–7] Typically, the catalytic activity of molecular WOCs is measured in a homogeneous aqueous medium using cerium(IV) (under acidic conditions) or tris(bipyridine)Ru(II) (under neutral conditions) as sacrificial oxidants, and a remarkably high turnover frequency (TOF) of 300 s^{-1} has been achieved very recently.[8] Moreover, accessible insight into mechanism and feasible structure modification of molecular WOCs surely enable further improvement in existing catalysts. However, for any implementation in an electrocatalytic or photoelectrocatalytic device toward water splitting, molecular WOCs have to be immobilized on the semi-conductive or conductive surface of an electrode.[9,10]

One of the major scientific challenges for WOCs immobilization is the requirement of a stable linking manner under harsh oxidizing conditions (the thermodynamic potential for water oxidation $E = 1.23 - 0.059 \times$ pH V *vs.* NHE). Reported approaches of tethering WOCs to the electrode surface mainly lie in two categories: one is covalent linkage through an ester type of bond formed between hydroxyl groups of the oxide surface and carboxylic or phosphoric groups of complexes;[11–13] the other is noncovalent linkage through electrostatic or π–π stacking interactions.[14–16] While the ester bond inevitably suffers from hydrolysis in aqueous surroundings, applications of noncovalent binding have certain limitations with respect to specific properties of electrode materials and catalysts. Herein, we would like to report a novel and widely applicable approach, by which molecular WOCs can be immobilized on conductive carbon surfaces *via* a strong covalent bond.

Our strategy consists of modifying catalysts with terminal acetylene groups on one hand, grafting azide-groups at the electrode surface on the other, and subsequently coupling the surface and WOCs *via* copper(I)-catalyzed azide–alkyne cycloaddition (so-called CuAAC or 'click') reaction, as depicted in Scheme 1a.[17] Advantages of this strategy includes: (1) the linkage between catalysts and surface is a robust triazole ring that is resistant to high oxidative potential and O_2-rich aqueous solutions; (2) CuAAC is a conveniently fast reaction even regarding heterogeneous coupling conditions. In the present work, a readily obtained glassy carbon (GC) disk electrode (∅ = 3 mm) was employed as a conductive platform, and a well-defined mononuclear Ru WOC, $[Ru^{II}(pdc)(pic)_3]$ (pdc = 2,6-pyridine-dicarboxylate, pic = 4-picoline), was chosen as a model complex to be immobilized.[5,18] It is important to note, however, that the strategy described here can be applied not only on GC and $[Ru^{II}(pdc)(pic)_3]$, but also on other carbon surfaces and various kinds of molecular WOCs.

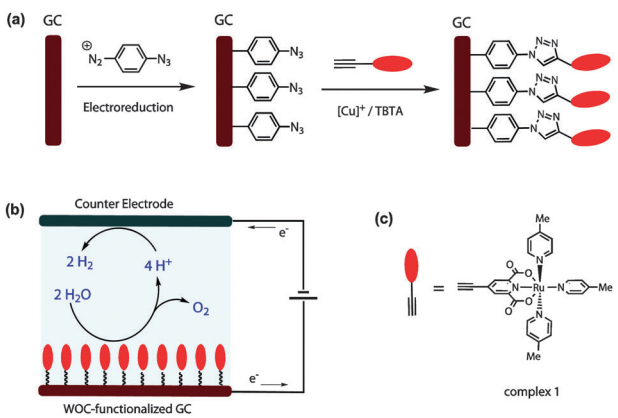

Scheme 1 Oxygen evolution at a functionalized GC surface. (a) Modification of the GC electrode with azide groups and coupling of ruthenium complex **1** by 'click' reaction. (b) Schematic illustration of a water-splitting electrochemical cell using functionalized GC as a working electrode. (c) Molecular structure of ruthenium WOC **1**.

[a] *Department of Chemistry, School of Chemical Science and Engineering, KTH Royal Institute of Technology, 100 44 Stockholm, Sweden. E-mail: lichengs@kth.se*
[b] *Department of Microelectronics and Applied Physics, School of Information and Communication Technology, KTH Royal Institute of Technology, 100 44 Stockholm, Sweden*
[c] *State Key Laboratory of Fine Chemicals, DUT-KTH Joint Education and Research Center on Molecular Devices, Dalian University of Technology (DUT), 116024 Dalian, China*

† Electronic supplementary information (ESI) available. See DOI 10.1039/c2cc35379b

The acetylene–substituted complex (**1** shown in Scheme 1c), as a derivative of $[Ru^{II}(pdc)(pic)_3]$, was developed by firstly substituting 4-H of pdc with trimethylsilylacetylene and affording 4-(trimethylsilyl)ethynylpyridine-2,6-dicarboxylic acid (H_2Tepc), secondly coordinating ruthenium with Tepc and pic ligands in one-pot reaction, and finally deprotecting TMS with $^{n}Bu_4N^+F^-$. The TMS group was used here in order to prevent any coordination between the Ru core and the terminal acetylene. Complex **1** was fully characterized by ^{1}H NMR,[13] C NMR, mass spectrometry and element analysis. Synthetic and spectroscopic details were provided in the ESI.† In principle, terminal acetylene can be installed to numerous types of ligands and complexes *via* facile synthetic chemistry.[19]

Reactive azide groups were grafted to the GC by direct electrochemical reduction of 4-azidobenzene diazonium tetrafluoroborate salt ($[N_3–C_6H_4–N_2]^+BF_4^-$) in 0.1 M HCl (a literature procedure was followed).[20] It is widely accepted that during the electrochemical reduction, an aryl radical generates from an aryl diazonium ion, attacks the carbon surface and forms a covalent C–C bond with the surface.[21] This process can be reflected from cyclic voltammogram (CV) curves of $[N_3–C_6H_4–N_2]^+BF_4^-$ recorded in 0.1 M HCl on a GC electrode (Fig. S3, ESI†). The first scan showed a broad irreversible wave at around −0.4 V *vs.* NHE, corresponding to the reductive potential of $[N_3–C_6H_4–N_2]^+BF_4^-$. At the second scan, however, the wave almost disappeared, indicating the block of the surface by the organic layer grafted to the surface. Besides GC, such an electrochemical grafting method has been successfully applied to a variety of carbon materials, like HOPG, carbon fibers and carbon nanotubes.[21,22]

Once the azide-modified GC and the acetylene-terminated WOC **1** were readily prepared, immobilization of the catalyst was carried out by simply immersing the modified electrode in a nonaqueous solution of **1** containing $[Cu(CH_3CN)_4]^+BF_4^-$ and TBTA as a typical condition for click chemistry. After a given incubation period, the catalyst-functionalized GC was copiously washed with acetone and ethanol, and then sonicated in acetone and ethanol, respectively, in order to remove any physically adsorbed complexes. The CV curves of catalyst-functionalized GC, recorded in the CH_2Cl_2 electrolyte, exhibit a reversible wave at 0.5 V *vs.* NHE (red line in Fig. 1). This redox potential is identical to the $E_{1/2}(Ru^{II}/Ru^{III})$ of $[Ru^{II}(pdc)(pic)_3]$ in a homogenous CH_2Cl_2 solution.[18] After multiple CV scans of the functionalized GC, the peak current of this characteristic redox potential did not show any discernible decay. Furthermore, the current peak was found to depend linearly on the scan rate from 20 to 500 mV s^{-1} with zero intercept (Fig. S5, ESI†), which is consistent with the behavior of surface-tethered redox couples. In contrast, no redox waves were observed in the CV curve of a control GC (black dash in Fig. 1), which is a pristine GC electrode treated using the same immobilization procedure as that for the azide-modified GC. These experiments clearly confirmed that WOC $[Ru^{II}(pdc)(pic)_3]$ was immobilized on the GC surface *via* a robust linkage, and a functionalized carbon surface $[Ru^{II}(pdc)(pic)_3]$@GC was yielded as we designed. Analysis of $[Ru^{II}(pdc)(pic)_3]$@GC by energy-dispersive X-ray spectroscopy (EDS) revealed a 0.12% weight percentage of ruthenium. By comparison, no weight percentage of ruthenium obviously higher than the background noise was detected in the EDS analysis of a pristine GC. The analyzed depth is on the order of 0.5 μm and the weight of the Ru at the surface is therefore small relative to the total mass.

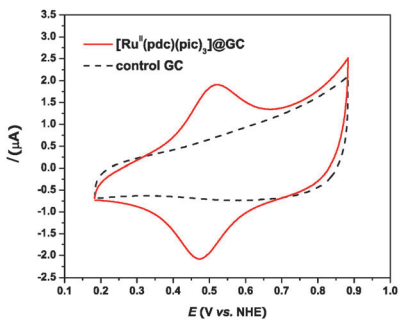

Fig. 1 CV curves of the $[Ru^{II}(pdc)(pic)_3]$ functionalized GC electrode (red line) and control GC electrode (black dash); conditions: 0.1 M $^{n}Bt_4N^+PF_6^-$ in CH_2Cl_2, scan rate = 100 mV s^{-1}, T = room temperature.

The effective coverage of WOC (Γ_0, mol cm^{-2}) on the $[Ru^{II}(pdc)(pic)_3]$@GC surface was estimated according to the linear relationship between the peak current of Ru^{II}/Ru^{III} and the scan rate (see ESI† for details). An average concentration of 1.2 ± 0.4 (10^{-10} mol cm^{-2}) was obtained from three independent experiments. Notably, this value can be significantly enhanced if a carbon electrode with a larger specific surface was used instead of GC.[20]

The electrocatalytic activity of $[Ru^{II}(pdc)(pic)_3]$@GC was first investigated by CV in a standard three-electrode cell consisted of a working electrode, a saturated calomel electrode (SCE) reference electrode and a platinum wire counter electrode (Scheme 1b). In a pH 7.0 phosphate buffer (IS = 0.1 M), the CV curve of $[Ru^{II}(pdc)(pic)_3]$@GC exhibits an onset of uprising current at about 1.25 V *vs.* NHE compared with the CV curve of a pristine GC (Fig. S7, ESI†), which is indicative of an electrocatalytic water oxidation on the $[Ru^{II}(pdc)(pic)_3]$@GC surface. This catalytic onset potential agrees with the electrocatalytic behavior of $[Ru^{II}(pdc)(pic)_3]$ in a homogeneous neutral aqueous medium, indicating retention of the catalytic activity of $[Ru^{II}(pdc)(pic)_3]$ after its immobilization.

The electrocatalytic activity of the $[Ru^{II}(pdc)(pic)_3]$@GC surface was further evaluated in a pH 7.0 phosphate buffer (IS 0.1 M) by chronoamperometric experiments, in which the current density of bulk electrolysis, either at a $[Ru^{II}(pdc)(pic)_3]$@GC or a pristine GC, was monitored continuously under a sequence of applied potential steps in the range from 1.1 to 1.5 V *vs.* NHE (shown in Fig. 2a and Fig. S9, ESI†). When the overpotential η—referred to an additional voltage to the thermodynamically required oxidative potential of water at pH 7.0 (E = 0.82 *vs.* NHE)—reaches 300 mV, an appreciable catalytic current was observed at a $[Ru^{II}(pdc)(pic)_3]$@GC in comparison with the current at a pristine GC (as a background). And the difference between current densities became quite significant at η = 500 mV, which implied a much more effective Faradaic process on the $[Ru^{II}(pdc)(pic)_3]$@GC surface, ascribed to an efficient catalytic water oxidation. The catalytic current density measured on $[Ru^{II}(pdc)(pic)_3]$@GC as a function of η followed a Tafel behavior that is displayed in the inset of Fig. 2b. Under the experimental conditions, the integral quantity of transferred

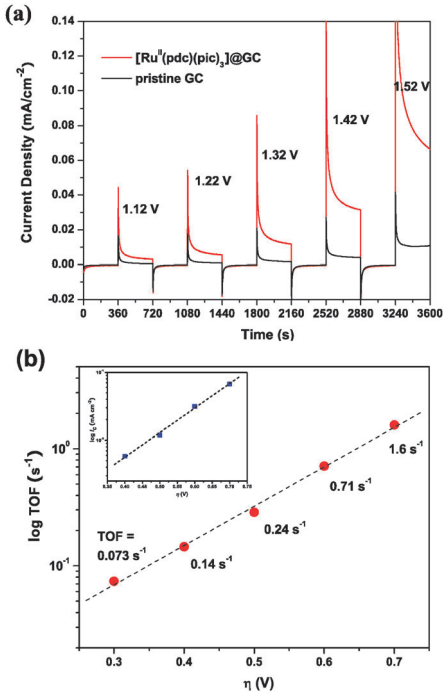

Fig. 2 Electroactivity of the $[Ru^{II}(pdc)(pic)_3]$ functionalized GC surface. (a) Chronoamperometric current density measured in potassium phosphate buffer (pH 7.0, IS = 0.1 M) at the $[Ru^{II}(pdc)(pic)_3]$@GC electrode (red trace) and the pristine GC electrode (black trace) under application of a sequence of potential steps shown in Fig. S8 (ESI†). (b) TOF plot of the $[Ru^{II}(pdc)(pic)_3]$ functionalized GC electrode as a function of overpotential η. The inset is a Tafel plot showing current density of the $[Ru^{II}(pdc)(pic)_3]$@GC surface *vs.* η.

electrons, assigned to catalytic water oxidation by immobilized $[Ru^{II}(pdc)(pic)_3]$, can be derived from the subtraction between the integrated charge through a $[Ru^{II}(pdc)(pic)_3]$@GC (Q_c, C cm^{-2}) and that through a pristine GC (Q_p, C cm^{-2}) during the integration time (t = 360 s) of given overpotential. Thus, the TOF of electroactive WOC on the $[Ru^{II}(pdc)(pic)_3]$@GC surface can be estimated by the following equation:

$$\mathrm{TOF} = \frac{1}{4} \times \frac{1}{t} \times \frac{(Q_c - Q_p)}{F\Gamma_0}$$

where F is Faraday's constant. Generation of every O_2 molecule includes extraction of four electrons from two H_2O molecules. The logarithm of yielded TOFs varies linearly on the applied overpotentials from 300 to 700 mV, as shown in Fig. 2b. This Tafel-like plot implicates a rate-determining step of electron transfer for O_2 evolution from the $[Ru^{II}(pdc)(pic)_3]$@GC surface. An initial TOF of 0.073 s^{-1} was achieved at η = 300 mV, which reaches 1.6 s^{-1} at η = 700 mV. Our previous study demonstrated that water oxidation by $[Ru^{II}(pdc)(pic)_3]$ occurred in a typical homogenous Ce^{IV}–CF_3SO_3H solution with a TOF of 0.23 s^{-1}.[5,18] Although the calculated TOF from $[Ru^{II}(pdc)(pic)_3]$@GC represented an upper bound of the realistic value, because Faradaic efficiency was assumed to be 100% in the calculation, the result emphasized a comparable, if not superior, catalytic activity of $[Ru^{II}(pdc)(pic)_3]$ on conductive surfaces in relation to homogeneous conditions.

In summary, our work herein provides a universal method, by which molecular WOCs can be firmly immobilized on conductive carbon surfaces, and meanwhile keep their catalytic activity at the hybrid interface. In principle, this method should be applicable to any molecular WOCs that can be modified with terminal acetylene groups. An employment of an engineered carbon electrode with large specific area, rather than GC, will significantly improve the concentration of WOC on the surface as well as promote catalytic current density in order of magnitude. Moreover, our strategy reported here is not limited by the size or specific properties of conductive carbon surfaces, which will inspire fabrication of an efficient water-splitting device in the context of exploitation of sustainable solar fuels.

We thank the Swedish Research Council, the K & A Wallenberg Foundation, the Swedish Energy Agency, the China Scholarship Council (CSC), the National Natural Science Foundation of China (21120102036) and the National Basic Research Program of China (2009CB220009) for financial support of this work.

Notes and references

1 J. Barber, *Chem. Soc. Rev.*, 2009, **38**, 185–196.
2 H. Dau, C. Limberg, T. Reiser, M. Risch, S. Roggan and P. Strasser, *ChemCatChem*, 2010, **2**, 724–761.
3 Y. Xu, A. Fischer, L. Duan, L. Tong, E. Gabrielsson, B. Åkermark and L. Sun, *Angew. Chem., Int. Ed.*, 2010, **49**, 8934–8937.
4 A. Sartorel, M. Carraro, G. Scorrano, R. D. Zorzi, S. Geremia, N. D. McDaniel, S. Bernhard and M. Bonchio, *J. Am. Chem. Soc.*, 2008, **130**, 5006–5007.
5 L. Duan, Y. Xu, M. Gorlov, L. Tong, S. Andersson and L. Sun, *Chem.–Eur. J.*, 2010, **16**, 4659–4668.
6 Q. Yin, J. M. Tan, C. Besson, Y. V. Geletii, D. G. Musaev, A. E. Kuznetsov, Z. Luo, K. I. Hardcastle and C. L. Hill, *Science*, 2010, **328**, 342–345.
7 J. L. Fillol, Z. Codolá, I. Garcia-Bosch, L. Gómez, J. J. Pla and M. Costas, *Nat. Chem.*, 2011, **3**, 807–813.
8 L. Duan, F. Bozoglian, S. Mandal, B. Stewart, T. Privalov, A. Llobet and L. Sun, *Nat. Chem.*, 2012, **4**, 418–423.
9 L. Duan, L. Tong, Y. Xu and L. Sun, *Energy Environ. Sci.*, 2011, **4**, 3296–3313.
10 P. D. Tran, V. Artero and M. Fontecave, *Energy Environ. Sci.*, 2010, **3**, 727–747.
11 Z. Chen, J. J. Concepcion, J. W. Jurss and T. J. Meyer, *J. Am. Chem. Soc.*, 2009, **131**, 15580–15581.
12 W. J. Youngblood, S.-H. A. Lee, Y. Kobayashi, E. A. Hernandez-Pagan, P. G. Hoertz, T. A. Moore, A. L. Moore, D. Gust and T. E. Mallouk, *J. Am. Chem. Soc.*, 2009, **131**, 926–927.
13 J. J. Concepcion, J. W. Jurss, P. G. Hoertz and T. J. Meyer, *Angew. Chem., Int. Ed.*, 2009, **48**, 9473–9476.
14 F. M. Toma, A. Sartorel, M. Iurlo, M. Carraro, P. Parisse, C. Maccato, S. Rapino, B. R. Gonzalez, H. Amenitsch, T. Da Ros, L. Casalis, A. Goldoni, M. Marcaccio, G. Scorrano, G. Scoles, F. Paolucci, M. Prato and M. Bonchio, *Nat. Chem.*, 2010, **2**, 826–831.
15 L. Li, L. Duan, Y. Xu, M. Gorlov, A. Hagfeldt and L. Sun, *Chem. Commun.*, 2010, **46**, 7307–7309.
16 F. Li, B. Zhang, X. Li, Y. Jiang, L. Chen, Y. Li and L. Sun, *Angew. Chem., Int. Ed.*, 2011, **50**, 12276–12279.
17 M. Meldal and C. W. Tornee, *Chem. Rev.*, 2008, **108**, 2952–3015.
18 L. Tong, Y. Wang, L. Duan, Y. Xu, X. Cheng, A. Fischer, M. S. G. Ahlquist and L. Sun, *Inorg. Chem.*, 2012, **51**, 3388–3398.
19 R. Chinchilla and C. Nájera, *Chem. Rev.*, 2007, **107**, 874–922.
20 D. Evrard, F. Lambert, C. Policar, V. Balland and B. Limoges, *Chem.–Eur. J.*, 2008, **14**, 9286–9291.
21 J. Pinson and F. Podvorica, *Chem. Soc. Rev.*, 2005, **34**, 429–439.
22 A. Le Goff, V. Artero, B. Jousselme, P. D. Tran, N. Guillet, R. Métayé, A. Fihri, S. Palacin and M. Fontecave, *Science*, 2009, **326**, 1384–1387.